

An experimentally justified confining potential for electrons in two-dimensional semiconductor quantum dots

Orion Ciftja

Received: 3 June 2006 / Accepted: 1 September 2006 / Published online: 16 February 2007
© Springer Science+Business Media B.V. 2007

Abstract We propose a confinement potential for electrons in a two-dimensional (2D) quantum dot that is more physically motivated and better experimentally justified than the commonly used infinite range parabolic potential or few other choices. Because of the specific experimental setup in a 2D quantum dot involving application of gate potentials, an area of electron depletion is created near the gate. The resulting positively charged region can be most simply modeled as a uniformly charged 2D disk of positive background charge. Within this experimental setup, the individual electrons in the dot feel a confinement potential originating from the uniformly positively charged 2D background disk. Differently from the infinitely high parabolic confinement potential, the resulting 2D charged disk potential has a finite depth. The resulting 2D charged disk potential has a form that can be reasonably approximated as a parabolic potential in the central region of the dot (for low energy states of the electrons) and as a Coulomb potential (that becomes zero at large distances). We study the electronic properties of the 2D charged disk confinement potential by means of the numerical diagonalization method and compare the results to the case of 2D quantum dots with a pure parabolic confinement potential.

PACS numbers 73.43.Cd · 73.20.Dx

Keywords Semiconductor quantum dots · Electron states · Confinement potential · Reduced dimensionality

1. Introduction

Semiconductor quantum dots are fabricated nanoscale systems in which charge carriers, such as electrons, are confined in a small region of space, usually, in two-dimensions (2D). The basic technological motivation to study quantum dots is to build nanoscale

O. Ciftja (✉)
Department of Physics, Prairie View A&M University, Prairie View, TX 77446, USA
e-mail: ogciftja@pvamu.edu

devices will fundamentally new properties that are smaller, faster, dissipate less heat and possess novel useful properties [1,2]. Confined electrons in a 2D semiconductor quantum dot show typical atomic properties [3] however, differently from real atoms, the confinement of electrons in a quantum dot is provided by an artificially created potential well that is not of Coulomb form. The most common theoretical model used to study 2D semiconductor quantum dots considers an isotropic parabolic confinement [4–11] and explains reasonably well some of the main features associated with common dots. Non-circular parabolic confinement potentials that are anisotropic have also been investigated [12,13]. Despite their wide use, both isotropic and anisotropic parabolic confinement models have limitations and are somehow inadequate because of the infinite range and infinite height of potential at large distances. In a real experiment and under given circumstances, such an assumption is clearly unphysical.

Although one cannot overlook the role of electronic correlations, the first step in understanding quantum dots is to study the single-particle aspects of the behavior of electrons under confinement. So far, the bulk of research has relied on the parabolic confining potential model with infinite range [14–18]. While this model is certainly appropriate at low energies, for instance quantum dots with few electrons, it is unsuitable to study larger quantum dots where a good number of electrons have higher energies and therefore are closer to the continuum threshold. Close to the continuum threshold, the shape of the confinement potential felt by electrons is no longer parabolic therefore an infinite range parabolic potential is no longer justified. To address this issue, few other potentials that do not become infinite at large distances have been proposed, among them a Gaussian [19] confining potential: $U(r) \propto -\exp(-c^2 r^2)$ and a smooth confining potential [20] of the form: $U(r) \propto -1/(c^2 + r^2)^2$. At small distances the above confining potentials are parabolic, while, at large distances they tend to a finite (zero) asymptotic value. While the above potentials do not have some of the shortcomings of the infinite range parabolic case, their physical origin and justification is far from being clear.

In this work, we propose a confinement potential for electrons in a 2D quantum dot that is better justified from an experimental point of view. The motivation for the choice comes from the consideration of the specific experimental setup in a 2D quantum dot. Such setup involves application of gate potentials who cause electron depletion in the area near the gates. The area depleted from electrons acts as a positively charged region which most simply can be modeled as a uniformly charged 2D disk with positive background charge. As a result, the confinement potential felt by individual electrons is the confinement potential originating from the uniformly positively charged 2D background disk. The 2D charged disk potential is different from the commonly used infinite range parabolic potential. At the bottom of the quantum well (in the central region of the disk) it has a parabolic form, however outside that region is no longer parabolic but behaves more like a Coulomb potential that obviously has a finite (zero) asymptotic value at large distances.

Here we present a study of the electronic structure of the finite depth 2D charged disk confinement potential. While the choice of other confinement potentials is somehow arbitrary the 2D charged disk confinement potential introduced here is experimentally justified and based on physics arguments. By using the exact numerical diagonalization approach we study the electronic structure and the bound energy spectrum corresponding to the finite charged disk potential. The current study is just a step forward on a more realistic representation of the quantum confinement problem on 2D semiconductor quantum dots.

2. The 2D charged disk confining potential

To derive the exact form of the 2D charged disk electrostatic confining potential, we first consider the interaction potential between an electron with charge, $-q_0 (q_0 > 0)$ and a uniformly charged finite 2D disk (the depleted region) with total positive charge Q and radius R . Both parameters, Q and R are experimentally controlled. It has been calculated [22] that the resulting electrostatic confining potential energy between an electron and a 2D charged disk can be written as:

$$U(r, R) = -q_0 V_0 F(r, R); \quad F(r, R) = \int_0^\infty \frac{dy}{y} J_0\left(\frac{r}{R}y\right) J_1(y), \tag{1}$$

where $F(r, R)$ is a function that depends only on the ratio r/R (given in integral form), $J_n(x)$ are n -th order Bessel functions, $r = \sqrt{x^2 + y^2}$ is the distance of the electron from the center of the disk, $V_0 = \frac{2kQ}{R}$ is the electrostatic potential created by the disk at its center ($r = 0$) and k is Coulomb's constant. Special values of this function are: $F(r = 0, R) = 1$ and $F(r = R, R) = 2/\pi$. The interaction potential, $U(r, R)/(q_0V_0) = -F(r, R)$ between an electron of charge $-q_0$ and the uniformly charged 2D disk with radius R is shown in Fig. 1 as a function of r/R . The suggestion to use confining potentials generated by charged disks has also been considered in an earlier work [21] where a two charge disk model was introduced. In this model, the basic electrostatic structure of a quantum dot was represented by two circular disks (of positive and negative charge) of radius R and homogeneous charge density σ_0 , vertically separated by a distance a . The radial potential (for $a < R$) in the electron layer was calculated to have the form:

$$\Phi(r, R, a) = \frac{2kNe}{R} \left[\sqrt{1 - \frac{a}{R}} - 1 + \frac{3}{8} \frac{a^2}{R^2} \frac{r^2}{R^2} - \frac{15}{32} \frac{a^4}{R^4} \frac{r^2}{R^2} + \frac{45}{128} \frac{a^2}{R^2} \frac{r^4}{R^4} + \dots \right], \tag{2}$$

where $Ne = \pi R^2 \sigma_0$ and $k = 1/(4\pi \epsilon_0)$. Differently from the two charge disk model, the confining potential, $U(r, R)$ proposed in the current work originates from a setup in which electrons are embedded in a single positively charged circular disk layer. Thus the positive background and electrons all belong to the same plane and are not vertically separated. Both potentials, $U(r, R)$ and $\Phi(r, R, a)$ (at finite a) have the same parabolic dependence $\propto r^2$ for small r . However, there are differences between confining potential $U(r, R)$ and the two charge disk model potential, $\Phi(r, R, a)$ most notably in the $a \rightarrow 0$ limit case where $\Phi(r, R, a \rightarrow 0) \rightarrow 0$.

As clearly seen in Fig. 1, the function $-F(r, R)$ is approximately parabolic for the whole range $0 \leq r \leq R$ and asymptotically becomes zero at large distances. While the integral presentation of $F(r, R)$ is rather convenient, the integral in Eq. 1 can also be carried out analytically [22] resulting in an expression of the form:

$$F(r, R) = \begin{cases} \frac{2}{\pi} E\left(\frac{r^2}{R^2}\right), & 0 \leq r \leq R \\ \frac{R}{2r} {}_2F_1\left(\frac{1}{2}, \frac{1}{2}, 2; \frac{R^2}{r^2}\right), & R \leq r < \infty, \end{cases} \tag{3}$$

where $E(z)$ is the complete elliptic integral of the second kind and ${}_2F_1(a, b, c; z)$ is the hypergeometric function [23].

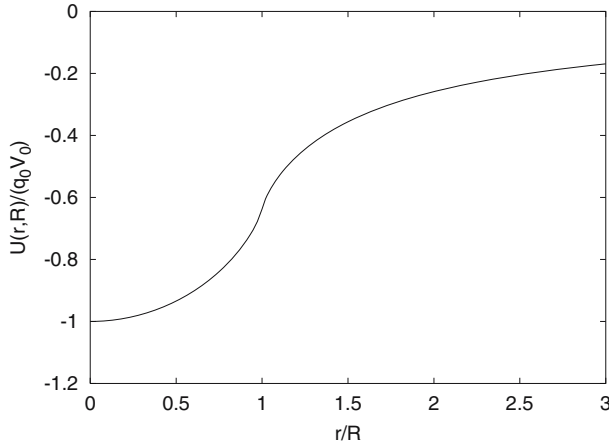


Fig. 1 The electrostatic interaction potential between an electron of charge $-q_0$ and the the uniformly charged 2D disk with radius R and charge Q . Here r is the distance of the electron from the center of the disk and $V_0 = 2kQ/R$ is the electrostatic potential of the uniformly charged disk at its center

Given that the exact interaction potential inside the disk closely resembles a parabolic function our first task is to find a reasonable parabolic approximation $U_p(r, R)$ and parametrize it. The simplest approach is to impose the constrains: $U_p(r = 0, R) = U(r = 0, R)$ and $U_p(r = R, R) = U(r = R, R)$, and as as result one obtains:

$$U_p(r, R) = -q_0 V_0 + c q_0 V_0 \left(\frac{r}{R}\right)^2; \quad c = 1 - \frac{2}{\pi} > 0. \tag{4}$$

With the mapping:

$$\frac{c q_0 V_0}{R^2} = \frac{m}{2} \omega^2, \tag{5}$$

the parabolic Hamiltonian corresponding to $U_p(r, R)$ immediately takes a standard 2D harmonic oscillator form:

$$\hat{H}_p = \frac{p^2}{2m} + U_p(r, R) = -q_0 V_0 + \frac{\hat{p}^2}{2m} + \frac{m}{2} \omega^2 r^2, \tag{6}$$

where m is the mass of the electron, ω is the resulting angular frequency [see Eq. 5] and \hat{p} is the linear momentum operator. The Hamiltonian corresponding to the realistic 2D charged disk confinement potential, $U(r, R)$ can be most conveniently written in terms of the parabolic Hamiltonian as:

$$\hat{H} = \hat{H}_p + \hat{H}'; \quad \hat{H}' = q_0 V_0 [1 - F(r, R)] - \frac{m}{2} \omega^2 r^2, \tag{7}$$

where \hat{H}' represents the departure from the parabolic model. In case perturbation theory is applied, \hat{H}' may be treated as a perturbation term acting on the 2D harmonic oscillator states.

3. Results and discussion

To simplify notation let us note: $\Delta\hat{H}_p = \hat{H}_p + q_0 V_0 = \frac{\hat{p}^2}{2m} + \frac{m}{2} \omega^2 r^2$ and $\Delta\hat{H} = \hat{H} + q_0 V_0 = \Delta\hat{H}_p + \hat{H}'$. To solve the Schrödinger equation corresponding to $\Delta\hat{H}$ we resort to the exact numerical diagonalization technique [24,25]. 2D harmonic oscillator states corresponding to $\Delta\hat{H}_p$ are used as an expansion basis. Since the quantum harmonic oscillator problem is found in many quantum mechanics textbooks we simply report that the energy eigenvalues corresponding to $\Delta\hat{H}_p$ are: $E_{n_r, l} = \hbar \omega (2 n_r + |l| + 1)$ where $n_r = 0, 1, \dots$ is the radial quantum number and $l = 0, \pm 1, \pm 2, \dots$ is the z -angular momentum quantum number. The normalized eigenfunctions corresponding to $\Delta\hat{H}_p$ are:

$$\Phi_{n_r, l}(r, \varphi) = \frac{e^{i l \varphi}}{\sqrt{2\pi}} R_{n_r, l}(r); \quad R_{n_r, l}(r) = N_{n_r, l}(\alpha r)^{|l|} e^{-\frac{\alpha^2 r^2}{2}} L_{n_r}^{|l|}(\alpha^2 r^2), \tag{8}$$

where $R_{n_r, l}(r)$ is the radial wave function, $L_{n_r}^{|l|}(\alpha^2 r^2)$ -s are associated Laguerre polynomials, $N_{n_r, l} = \sqrt{\frac{2 n_r! \alpha^2}{(n_r + |l|)!}}$ is a normalization constant and $\alpha = \sqrt{\frac{m \omega}{\hbar}}$ is the common harmonic oscillator parameter that has the dimensionality of an inverse length. We recall that the Hamiltonian corresponding to the 2D charged disk confinement potential is: $\hat{H} = \hat{H}_p + \hat{H}'$ (or $\Delta\hat{H} = \Delta\hat{H}_p + \hat{H}'$). A numerical solution of the stationary Schrödinger's equation corresponding to \hat{H} (or $\Delta\hat{H}$) is achieved by using the exact diagonalization technique where 2D oscillator eigenstates are used as basis functions. To set up the Hamiltonian matrix, we must calculate the matrix elements of $\Delta\hat{H}$ in the $\{|n_r, l\rangle\}$ basis of 2D harmonic oscillator states. Non-diagonal terms arise only from the \hat{H}' operator which is diagonal with respect to l but not n_r . For a given value of the angular momentum, l we have: $\langle n'_r, l | \Delta\hat{H} | n_r, l \rangle / (\hbar \omega) = (2 n_r + |l| + 1) \delta_{n'_r, n_r} + h_{n'_r, n_r}$ where $h_{n'_r, n} = \langle n'_r, l | \hat{H}' | n_r, l \rangle / (\hbar \omega)$ and energies are measured in $\hbar \omega$ units. It is straightforward to calculate:

$$h_{n'_r, n_r} = \frac{1}{2} \sqrt{\frac{n'_r! n_r!}{(n'_r + |l|)! (n_r + |l|)!}} \int_0^\infty dt t^{|l|} e^{-t} L_{n'_r}^{|l|}(t) L_{n_r}^{|l|}(t) \times \left\{ \frac{(\alpha R)^2}{c} [1 - F(\sqrt{t}, \alpha R)] - t \right\}, \tag{9}$$

where the auxiliary variable $t = \alpha^2 r^2$ was introduced to simplify calculations. For chosen z -angular momentum values, $l = 0, \pm 1, \dots$ we build sufficiently large Hamiltonian matrices and solve the eigenvalue–eigenstate problem by means of standard diagonalization methods. For any given (dimensionless) disk radius, αR , the smallest of the energy eigenvalues represents the ground state energy. Since the main focus is on the bound energy states of the 2D charged disk confinement potential

we choose $\alpha R = 3$ for the disk radius. This value results in a quantum well with depth: $-q_0 V_0 / (\hbar \omega) = -(\alpha R)^2 / (2c)$ which roughly guarantees to accomodate more than ten electrons. In Fig. 2 we show the resulting bound energy spectrum for the 2D charged disk potential $U(r, R)$ (in dimensionless harmonic oscillator energy units and measured with respect to the bottom of the well $-q_0 V_0 / (\hbar \omega)$) for selected z -angular momentum values, $|l| = 0, \dots, 10$ and for $\alpha R = 3$. Since the accuracy of results from expansions in a finite basis is usually best for the lowest energy states and deteriorates with increasing energy, the energy spectrum close to the continuum threshold is less accurate than the spectrum close to the bottom of the finite quantum well. As clearly seen in Fig. 2 the general effect of the 2D charged disk potential compared to the 2D parabolic potential is a lowering of the corresponding oscillator eigenenergies. Such effect becomes more pronounced for higher eigenenergies closer to the continuum threshold. Closer to the continuum threshold the eigenenergies corresponding to the 2D charged disk are also more closely packed than the parabolic counterpart resulting in a higher density of states. In Fig. 3 we plot the ground state and an excited state

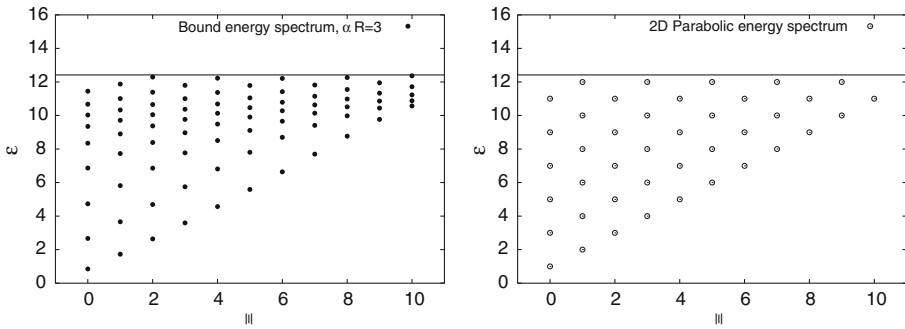


Fig. 2 Bound energy spectrum, $\epsilon = \langle \Delta \hat{H} \rangle / (\hbar \omega)$ for the electron with charge $-q_0$ in the confining potential, $U(r, R)$ for $\alpha R = 3$. The solid circles represent the bound energies corresponding to each z -angular momentum quantum numbers, $|l| = 0, \dots, 10$. The solid line represents the depth, $q_0 V_0 / (\hbar \omega)$ of the confining well [left]; The equivalent energy spectrum corresponding to the 2D parabolic confinement potential [right]

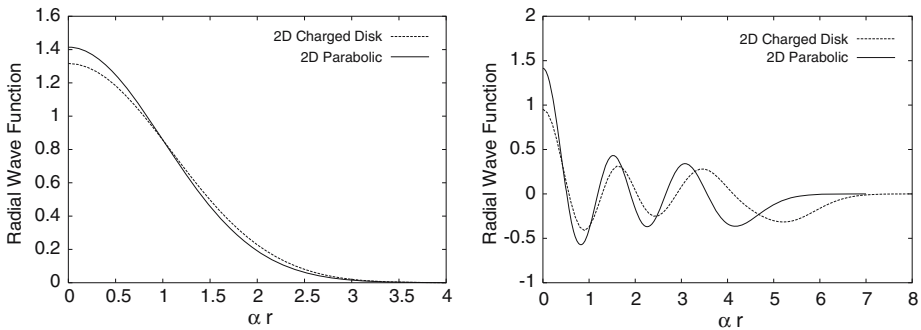


Fig. 3 Ground state radial wave function ($n = 0, |l| = 0$) for the 2D parabolic confining potential (solid line) and for the 2D charged disk confining potential (dashed line) [left]; An excited state radial wave function ($n = 5, |l| = 0$) closer to the continuum threshold for the 2D parabolic confining potential (solid line) and the corresponding state for the 2D charged disk confining potential (dashed line) [right]

(rather close to the continuum threshold) radial wave function for a 2D charged disk confining potential with radius $\alpha R = 3$ and compare the result to the corresponding 2D parabolic radial wave functions. While the two ground state wave functions are very similar (for low energy states the 2D charged disk potential is approximately parabolic) this is not the case for higher excited energy states. Closer to the continuum threshold the excited state wave functions of the 2D charged disk potential spread out much more than the parabolic counterparts. For relatively large quantum dots, a sizeable number of bound electrons have their energies close to the continuum threshold therefore under this scenario the parabolic model is a rather poor representation. In particular, for the case of **laterally coupled** quantum dots, such as double quantum dots [26–28] an infinite range parabolic confinement model cannot be used since it does not allow unbounding of states from individual harmonic wells. The introduction of finite range cut-offs on individual dot potentials or the consideration of M -minima confinement potentials [29] of the form: $U(r) = \frac{m}{2} \omega^2 \min \left[\sum_{j=1}^M (\vec{r} - \vec{L}_j)^2 \right]$, while allowing inter-dot tunneling cannot be fully justified from the theoretical point of view. When considering relatively large dots and for electrons with energies close to the continuum threshold ($r \gg L_j$) this confinement potential behaves exactly like the infinitely high parabolic potential therefore suffers from the same unphysical limitations.

On the other hand, the 2D charged disk confining potential introduced here is fully justified from the theoretical point of view. Consistent with all experiments, it is parabolic at low energy states (dots with few electrons localized in the center of the trap) and decays smoothly for higher energy states (for larger dots with more electrons on the edges of the trap having energies closer to the continuum threshold). Given that the 2D charged disk potential decays smoothly (unlike the parabolic potential that increases quadratically with distance), it naturally allows “leaking” of electrons from the interior of the dot therefore is ideally suited to model systems of laterally coupled quantum dots without resorting to further assumptions. For a given system of laterally coupled quantum dots the overall confinement potential would be a combination of individual 2D charged disk potentials. The net result is a confinement potential with multi-minima that allows inter-dot tunneling and does not become infinite far away from the central trapping regions.

Acknowledgements We wish to acknowledge the support by the U.S. D.O.E. (Grant No. DE-FG52-05NA27036).

References

1. Jacak, L., Hawrylak, P., Wojs, A.: Quantum Dots. Springer, Berlin (1997)
2. Tarucha, S., Austing, D.G., Honda, T., van der Hage, R.J., Kouwenhoven, L.P.: Shell filling and spin effects in a few electron quantum dot. *Phys. Rev. Lett.* **77**, 3613–3616 (1996).
3. Ashoori, R.C., Stormer, H.L., Weiner, J.S., Pfeiffer, L.N., Baldwin, K.W., West, K.W.: N-electron ground state energies of a quantum dot in magnetic field. *Phys. Rev. Lett.* **71**, 613–616 (1993).
4. Maksym, P.A., Chakraborty, T.: Quantum dots in a magnetic field: Role of electron-electron interactions. *Phys. Rev. Lett.* **65**, 108–111 (1990).
5. Merkt, U., Huser, J., Wagner, M.: Energy spectra of two electrons in a harmonic quantum dot. *Phys. Rev. B* **43**, 7320–7323 (1991).
6. Pfannkuche, D., Gerhardt, R.R.: Quantum-dot helium: Effects of deviations from a parabolic confinement potential. *Phys. Rev. B* **44**, 13132–13135 (1991).
7. MacDonald, A.H., Johnson, M.D.: Magnetic oscillations of a fractional Hall dot. *Phys. Rev. Lett.* **70**, 3107–3110 (1993).

8. Pfannkuche, D., Gudmundsson, V., Maksym, P.A.: Comparison of a Hartree, a Hartree-Fock, and an exact treatment of quantum-dot helium. *Phys. Rev. B* **47**, 2244–2250 (1993).
9. Yannouleas, C., Landman, U.: Collective and independent-particle motion in two-electron artificial atoms. *Phys. Rev. Lett.* **85**, 1726–1729 (2000).
10. Tavernier, M.B., Anisimovas, E., Peeters, F.M.: Correlation between electrons and vortices in quantum dots. *Phys. Rev. B* **70**, 155321-1–155321-8 (2004).
11. Tavernier, M.B., Anisimovas, E., Peeters, F.M., Szafran, B., Adamowski, J., Bednarek, S.: Four-electron quantum dot in a magnetic field. *Phys. Rev. B* **68**, 205305-1–205305-9 (2003).
12. Drouvelis, P.S., Schmelcher, P., Diakonov, F.K.: Probing the shape of quantum dots with magnetic fields. *Phys. Rev. B* **69**, 155312-1–155312-5 (2004).
13. Drouvelis, P.S., Schmelcher, P., Diakonov, F.K.: Two-electron anisotropic quantum dots. *Europhys. Lett.* **64**, 232–238 (2003).
14. Maksym, P.A.: Eckardt frame theory of interacting electrons in quantum dots. *Phys. Rev. B* **53**, 10871–10886 (1996).
15. Bolton, F.: Fixed-phase quantum Monte Carlo method applied to interacting electrons in a quantum dot. *Phys. Rev. B* **54**, 4780–4793 (1996).
16. Kainz, J., Mikhailov, S.A., Wensauer, A., Rössler, U.: Quantum dots in high magnetic fields: Calculation of ground state properties. *Phys. Rev. B* **65**, 115305-1–115305-5 (2002).
17. Harju, A., Siljamäki, S., Nieminen, R.M.: Wigner molecules in quantum dots: A quantum Monte Carlo study. *Phys. Rev. B* **65**, 075309-1–075309-6 (2002).
18. Partoens, B., Peeters, F.M.: Molecule-type phases and Hund’s rule in vertically coupled quantum dots. *Phys. Rev. Lett.* **84**, 4433–4436 (2000).
19. Adamowski, J., Sobkowicz, M., Szafran, B., Bednarek, S.: Electron pair in a Gaussian confining potential. *Phys. Rev. B* **62**, 4234–4237 (2000).
20. De Filippo, S., Salerno, M.: Spectral properties of a model potential for quantum dots with smooth boundaries. *Phys. Rev. B* **62**, 4230–4233 (2000).
21. Stopa, M.: Quantum dot self-consistent electronic structure and the Coulomb blockade. *Phys. Rev. B* **54**, 13767–13783 (1996).
22. Ciftja, O., Wexler, C.: Monte Carlo simulation method for Laughlin-like states in a disk geometry. *Phys. Rev. B* **67**, 075304-1–075304-8 (2003).
23. For the definition of complete elliptic integral of the second kind and hypergeometric functions, see Chapter 5 and Chapter 13 of: *Mathematical Methods For Physicists*, Fifth Edition, George B. Arfken and Hans J. Weber, Academic Press (2001).
24. Ciftja, O., Anil Kumar, A.: Ground state of two-dimensional quantum-dot helium in zero magnetic field: Perturbation, diagonalization, and variational theory. *Phys. Rev. B* **70**, 205326-1–205326-8 (2004).
25. Ciftja, O., Faruk, M.G.: Two-dimensional quantum-dot helium in a magnetic field: Variational theory. *Phys. Rev. B* **72**, 205334-1–205334-10 (2005).
26. Petta, J.R., Johnson, A.C., Yacoby, A., Marcus, C.M., Hanson, M.P., Gossard, A.C.: Pulsed-gate measurements of the singlet-triplet relaxation time in a two-electron double quantum dot. *Phys. Rev. B* **72**, 161301-1–161301-4(R) (2005).
27. A. C. Johnson, J. R. Petta, C. M. Marcus, M. P. Hanson, and A. C. Gossard, Singlet-triplet spin blockade and charge sensing in a few-electron double quantum dot. *Phys. Rev. B* **72**, 165308-1–165308-7 (2005).
28. Mourokh, L.G., Smirnov, A.Y.: Negative differential conductivity and population inversion in the double-dot system connected to three terminals. *Phys. Rev. B* **72**, 033310-1–033310-4 (2005).
29. Helle, M., Harju, A., Nieminen, R.M.: Two-electron lateral quantum-dot molecules in a magnetic field. *Phys. Rev. B* **72**, 205329-1–205329-24 (2005).